Nonlinear Seismic Wave Propagation in Heavy Oil

Wubing Deng and Igor B. Morozov
University of Saskatchewan

Summary

The propagation, reflectivity, and attenuation of seismic waves in bitumen-rich rocks and heavy oils can be difficult to explain by the traditional viscoelastic concepts, such as the *Q* factor. Heavy oils are likely non-Newtonian, and both viscosity and elasticity in them can be nonlinear. Recent lab experiments with Crisco vegetable shortening (Lines et al., Geophysical Prospecting, 2014) produced several remarkable observations useful for understanding such media: 1) low amplitudes and 2) low dominant frequencies of propagating waves, and 3) very strong negative reflectivity in water. Here, we propose a nonlinear model explaining these observations. The Crisco is interpreted as a viscous (Voigt) solid/fluid with strongly nonlinear behaviour at high strains. This nonlinearity affects a narrow zone extending to 1-2 wavelengths from the source or from the water-Crisco boundary. This zone is responsible for all three key effects listed above. Beyond this zone, wave propagation is near-linear and similar to that in Crisco altered by melting and re-solidification. Notably, the reflections from unaltered Crisco in water are strong and of negative polarity, showing that they are caused by a dynamically-reduced effective modulus. By contrast, reflections from altered Crisco are much weaker and phase-rotated, which suggests that they are caused by contrasts in viscosity. Thus, physical properties such as nonlinear moduli and viscosity (and not so much the *Q*) provide a good way for explaining the behaviour of seismic waves in viscous-fluid rich or fluid-like solids.

Introduction

When considering wave propagation and reflectivity in weakly attenuative media or corrections for attenuation effects in seismic data processing, the quality factor (*Q*) is a convenient property representing the internal friction within materials (Lines et al., 2008; Reine et al. 2012; van der Baan, 2012; Lines, et al. 2014). The use of *Q* allows modeling the observed attenuation effects, and it is relatively easy to implement in numerical algorithms (e.g., Zhu, et al. 2013). However, for media with strong dissipation, such as viscous, heavy oil, specifying the *Q* alone is incomplete and insufficient for describing the behavior of seismic waves. In such cases, one needs to look into a more complete physical picture and identify the true physical parameters responsible for seismic attenuation.

The difficulties of the conventional *Q*-based model can be demonstrated on the recent results of ultrasonic measurements of acoustic wave propagation and reflections in Crisco (Wong and Lines, 2013 and Lines et al. 2013). Crisco is a popular solidified (hydrogenated) vegetable shortening used to test acoustic-wave effects in viscous oils in the lab. Wong and Lines (2013) measured the reflectivity of the water-Crisco contact and found it to be of negative-polarity and surprisingly strong, close to about (-0.7). This result could be explained neither by the difference in impedances (ρV, which is very small for Crisco and water) nor by the effect of a very low *Q* (which would cause a 90°-rotated reflection; Lines et al., 2014). In addition, the very low *Q* (~0.3 to 3) required for such reflectivity would also disagree with the observations of direct waves in Crisco, which only suggest moderate *Q* values of ~15–50 (Wong and Lines, 2013).

Another rarely noted limitation of the *Q* model is in its disagreement with poroelasticity (Biot, 1956). The frictional stress field in a poroelastic medium is proportional to filtration velocities, whereas in order to be described by a *Q*, the stress must be proportional to the strain and/or strain rate. However, poroelastic effects should likely play some role in the behavior of fluid-saturated and bitumen-rich rocks. All this suggests that the physics of wave attenuation in Crisco (and therefore likely in heavy oils) does not easily reduce to the *Q*-type phenomenology.

Here, we try explaining the disagreements in Crisco experiments mentioned above by testing a broader model of nonlinear viscosity and elasticity. In this model, there is no unique *Q* parameter, and this parameter is not needed for modeling wave attenuation effects. The observed frequency dependences of the wave *Q*s and effective moduli are explained by the dependences of the viscosities and elastic constants on strains and strain rates within the wave. This model is therefore fully consistent with mechanics and thermodynamics. We show how this model explains all experiments with both unaltered and altered Crisco (Wong and Lines, 2013) and constrain several physical parameters of this medium.

Method

Similarly to fluids, solids possess viscosity. This property means that in a deformed body, there exist stresses dependent on the strain rate (Landau and Lifshitz, 1986). In a Newtonian solid, the stress-strain relation contains two parts: 1) the elastic stress-relation (Hooke's law):

$$\sigma_{ij}^{\mathrm{el}} = \lambda \frac{\partial u_k}{\partial x_k} \delta_{ij} + \mu \left(\frac{\partial u_i}{\partial x_j} + \frac{\partial u_j}{\partial x_i} \right), \tag{1}$$

and 2) viscous stress with a similar dependence on strain rates (Naviér-Stokes law):

$$\sigma_{ij}^{\mathrm{visc}} = \lambda' \frac{\partial \dot{u}_k}{\partial x_k} \delta_{ij} + \mu' \left(\frac{\partial \dot{u}_i}{\partial x_j} + \frac{\partial \dot{u}_j}{\partial x_i} \right). \tag{2}$$

In equations (1) and (2), u_i, is the displacement λ and μ are the Lamé constants, and the overdot indicates the time derivatives. Parameters λ' and μ' are analogous to μ and λ and represent the 'dynamic' (ordinary, or shear) and 'second' viscosities, respectively. The combined stress laws (1) and (2) describe the medium known as the Voigt solid (Kolsky, 1963). This is the simplest model of viscous friction within an isotropic solid without knowledge or assumptions about its internal structure (Landau and Lifshitz, 1986).

Substitution of stresses (1) and (2) in the second Newton's law gives the equation of motion for the Voigt solid:

$$\rho \ddot{u}_i = \left(\sigma_{ij}^{\mathrm{el}} + \sigma_{ij}^{\mathrm{visc}} \right)_{,j} + f_i \,. \tag{3}$$

Equations (1) – (3) describe wave propagation in linear anelastic media. In the derivation of these equations, no notions of 'relaxation mechanisms' are used and only rigorous principles of physics are followed.

For constant $(\lambda,\ \mu)$ and (λ', μ'), equations (1)–(2) are linear with respect to deformation magnitude. Heavy oils, however, are most likely non-Newtonian fluids, and bitumen-rich rocks may also exhibit nonlinear elastic properties, especially in the near-source regions of strong amplitudes. Minster et al. (1991) considered such nonlinear effects on the near-source attenuation, by assuming a dependence of the material *Q* on the strain. Coulman et al. (2013) proposed a power-law nonlinear viscosity for modeling the observed frequency-dependent *Q* spectra measured in lab experiments. In our approach, the nonlinearity arises naturally by noting that the elastic parameters λ and μ can depend on the strain, and parameters λ' and μ' in (2) can depend on both the strain and strain rate.

From a recent interpretation of the measurements with Crisco (Morozov et al, in preparation), all observations by Wong and Lines (2013) can be explained by allowing different levels of material constants λ, μ, λ', and μ' for low and high levels of strain, separated by some strain threshold ε_0. Such dependences can be modeled by using a sigmoid function $s(x) = \left[1 + \exp(-6x)\right]^{-1}$ (Figure 1):

$$p(x) = p_{low} + \left(p_{high} - p_{low}\right) S\left(\frac{|\varepsilon|}{\varepsilon_0} - 1\right), \tag{4}$$

where ε_0 is the strain level at which the transition from p_{low} to p_{high} occurs, and parameter *p* represents either the modulus or viscosity in this expression. For simplicity, for viscosity parameters λ' and μ', we only consider dependences on the combined strain and strain-rate magnitude, defined by $\tilde{\varepsilon} \equiv \sqrt{(\dot{\varepsilon}\tau)^2 + \varepsilon^2}$. For the numerical examples below, we also (arbitrarily) take the time constant τ in this relation equal 1 μs.

Numerical Modeling

Let us consider propagation of a *P* wave in Crisco based on laboratory measurements by Wong and Lines (2013). For *P* waves, the elastic constants in eqs. (1) and (2) are combined into the *P*-wave modulus $M = \lambda + 2\mu$ and the corresponding viscosity $\eta = \lambda' + 2\mu'$. As discussed in detail by Morozov et al. (in preparation), the observations for unaltered and altered Crisco can be explained by the following values of these material parameters:

1) For unaltered Crisco, the strain-dependent modulus M ranges from 0.2 GPa for high strains to 2.5 GPa for low strains. The strain-dependent viscosity η varies from 51 Pa·s for low strains to 78 Pa·s for high strains (Figure 1).
2) For altered Crisco, the modulus M ranges from 2.09 GPa for high strains to 2.32 GPa for low strains. The viscosity η varies from 16 Pa·s for low strains to 39 Pa·s for high strains.

The time-domain differential equations (1)–(3) can be readily implemented in 1-D a finite-difference algorithm. The source is modelled as a zero-phase Ricker wavelet with dominant frequency 800 kHz. Because of the nonlinearity an high η/M ratio near the source, the peak frequency drops within about two wavelengths, after which the peak frequencies drop to ~500 kHz and ~250 kHz for the altered- and unaltered- Crisco respectively. These frequencies are close to those observed for direct waves and reflections (Wong and Lines, 2013).

Figure 2 compares the direct-wave waveforms modeled in unaltered and altered Crisco. Note that the waves decay in amplitudes and have dispersive shapes. Interestingly, the shapes of the 'far-field' wavelets are strongly different in these two cases. The wavelet in altered Crisco is similar to the zero-phase source wavelet, whereas the wavelet in unaltered Crisco is strongly phase-rotated. This rotation occurs within a thin near-source zone of very high nonlinear attenuation. This zone extends to ~1–2 wavelengths from the source or water-Crisco boundary, after which the strain drops and the propagation and attenuation become linear and correspond to the low-strain regime (Figure 1).

Figure 3 shows the attenuation rates (Q^{-1}), as functions of strain amplitudes, for harmonic waves modeled in unaltered and altered Crisco at three different frequencies. When strains are high, $\varepsilon > \varepsilon_0$, the levels of Q^{-1} are also high and show strong variation with frequency. For low strains $\varepsilon < \varepsilon_0$, Q^{-1} is much lower. This is the far-field regime. In this regime, the Q^{-1} of both unaltered and altered Crisco are similar.

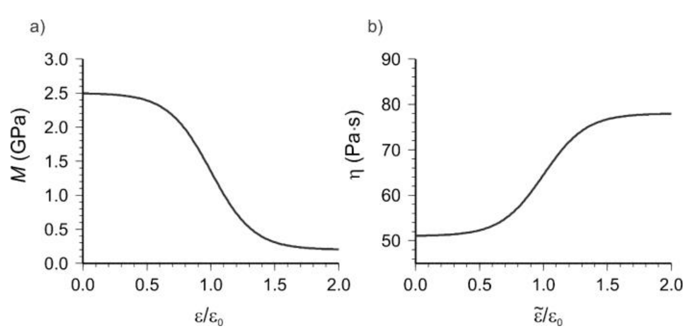

Figure 1. Schematic nonlinear strain-dependent model for unaltered Crisco: a) Strain dependence of the P-wave modulus *M*; b) Dependence of P-wave viscosity η on the combined strain and strain-rate magnitude.

In the near field, the plane-wave attenuation in unaltered Crisco at 800 kHz is ~30–40 times higher than that in altered Crisco and corresponds to $Q \approx 0.8$. This ultra-low Q causes a rapid decay of the amplitude, a drop in the peak frequency, and a phase rotation within the near-source zone, causing the observed much lower amplitudes and dominant frequencies in the 'far field' in (Wong and Lines, 2013).

Figure 4 compares reflections from three different interfaces, which are also very close to those observed in the experiments by Wong and Lines (2013). The particle displacements of the reflections from water-unaltered Crisco contact are almost the same in magnitude but of opposite polarity compared to those from aluminum (Figure 4). This opposite polarity is caused by the very low elastic modulus of the thin boundary of the unaltered Crisco ($M \approx 0.2$ GPa at high strain). Therefore, the nonlinear modulus here dominates the reflectivity. However, the viscosity difference also contributes to the wavelet shape variations (red line in Figure 4).

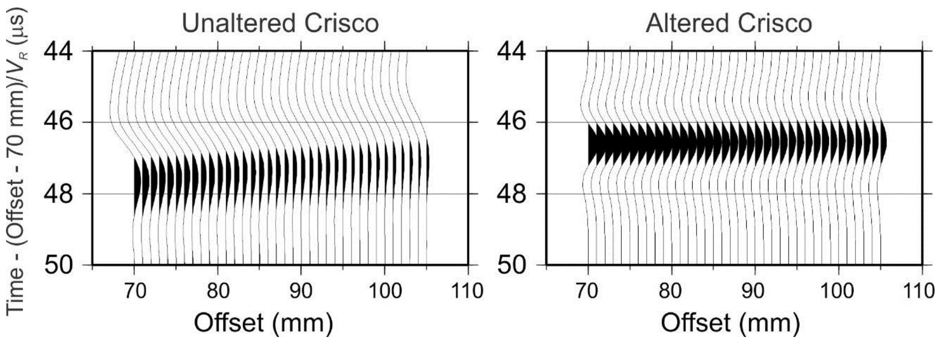

Figure 2. Direct-wave waveforms in unaltered and altered Crisco simulated by finite-difference modeling. Linear travel-time moveout with velocity V_R = 1540 m/s is removed.

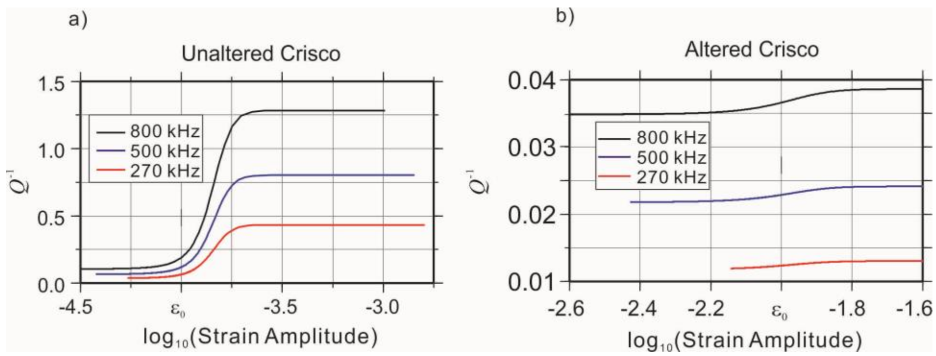

Figure 3. Frequency and strain-dependent nonlinear attenuation. a) Q^{-1} spectrum of unaltered Crisco with $\varepsilon_0 = 10^{-4}$, while b) is the Q^{-1} spectrum of altered Crisco with $\varepsilon_0 = 10^{-2}$.

The altered Crisco has a narrow (interpreted) variation of the modulus (from 2.09 to 2.32 GPa), which is very close to that of water. The model shows small amplitude reflections from the water-altered Crisco contact (blue line in Figure 4). Unlike the reflection from water-unaltered Crisco contact, the reflection from altered Crisco shows a nearly 90° phase shift (blue line in Figure 4). Such phase-rotated reflection is controlled by the viscosity contrast. Note that similarly, strong nonlinear viscosity causes phase-rotated direct waves in unaltered Crisco (Figure 2).

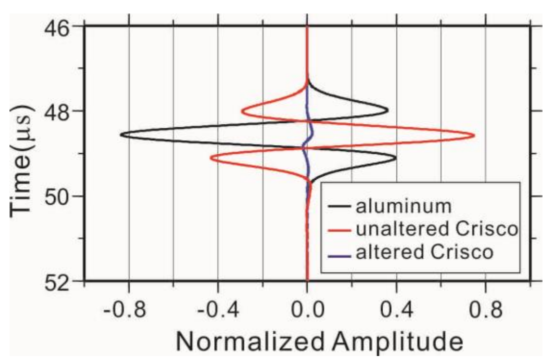

Figure 4. Displacement seismograms modeled for different media in contact with water. Black line respects to reflection from water-aluminum contact, red line denotes reflection from water-unaltered Crisco contact and blue line represents that from water-altered Crisco contact.

Discussion

The modeling described above successfully explains all three key observations with unaltered and altered Crisco by Wong and Lines (2013): 1) the amplitudes and attenuation of direct waves, 2) reduction of dominant frequencies; and 3) reflection amplitudes in water. The physical, nonlinear viscosity-based approach provides us a new understanding of heavy-oil-like media.

However, both this modeling and lab experiments were conducted at ultrasonic frequencies. Because of the nonlinearity, and also because of strong attenuation and dispersion of waves in viscous media, transferring these results to exploration seismic frequencies can be highly challenging. Further research of this subject is definitely required.

Conclusions

Recent laboratory observations of acoustic wave propagation and reflectivity in a proxy for heavy oil (Crisco; Wong and Lines, 2013) can be explained by nonlinear elasticity and viscosity. The nonlinearity concentrates in a narrow range of about 1-2 wavelengths near the source, where high strains ($\varepsilon > \varepsilon_0$) occur. The attenuation rate within this zone can be very high, causing a drop in the amplitude and peak frequency of the signal, and a phase rotation of the wavelet. Beyond this nonlinear range, the attenuation rate decreases, and wave propagation becomes linear. Modeling of reflections indicates that reflectivity from unaltered and altered (melted and re-solidified) Crisco in water occur differently. The strong negative reflections observed from unaltered Crisco are mainly due to the nonlinear reduction of the elastic modulus under high strain. For altered Crisco, the reflectivity is phase-rotated and principally explained by a contrast in viscosity.

Acknowledgements

This study was supported in part by Canada NSERC Discovery Grant RGPIN261610-03. W. D. was supported by the Scholarship Council, People's Republic of China.

References

van der Baan, M., 2012, Bandwidth enhancement: Inverse Q filtering or time-varying Wiener deconvolution?: Geophysics 77, V133-V142, doi: 10.1190/geo2011-0500.1.

Biot, M. A., 1956, Theory of propagation of elastic waves in a fluid-saturated porous solid. I. Low-frequency range. The Journal of the Acoustical Society of America 28: 168, doi: 10.1121/1.1908239.

Reine, C., R. Clark, M. van der Baan, 2012, Robust prestack Q-determination using surface seismic data: Part 1 — Method and synthetic examples: Geophysics, 77, R45-R56, doi: 10.1190/geo2011-0073.1.

Coulman, T., W. Deng, and I. B. Morozov, 2013, Models of seismic attenuation measurements in the laboratory: Canadian Journal of Exploration Geophysics, 38, 51-67.

Kolsky, H., 1963. Stress waves in solids, Dover Publications.

Lines, L., F. Vasheghani, and S. Treitel, 2008, Reflections on Q: CSEG Recorder 34: 36-38.

Landau, L. and E. Lifshitz, 1986, Theory of elasticity, Pergamon Press, Oxford: 155.

Lines, L., J. Wong, K. Innanen, F. Vasheghani, C. Sondergeld, S. Treitel, and T. Ulrych, 2014, Research Note: Experimental measurements of Q-contrast reflections: Geophysical Prospecting, 62, 190-195, doi: 10.1111/1365-2478.12081.

Minster, J. B., Day, M. Steven, and P. M. Shearer, 1991, The transition to the elastic regime in the vicinity of an underground explosion: American Geophysical Union, 65, 229-238.

Morozov, I. B., W. Deng, L. Lines, C. Sondergeld, and S. Treitel, Seismic wave propagation and reflections in highly attenuative media, in preparation for Geophysical Prospecting

Wong, J., and L. Lines, 2013, Physical modeling of reflections from low-Q media: Canadian Journal of Exploration Geophysics, 38, 32-39.

Zhu, T., J. M. Carcione, and J.M. Harris, 2013, Approximating constant-Q seismic propagation in the time domain: Geophysical Prospecting, 61, 931 – 940, doi: 10.1111/1365-2478.12044.